

Original Article

Prognostic and immunological roles of RSP01 in pan-cancer and its correlation with LUAD proliferation and metastasis

Xinqi Lou^{1*}, Yuanyuan Wang^{2*}, Yanjun Deng², Jiao Yang¹, Duo Xu², Mingdeng Wang², Yuansheng Lin²

¹Institute of Clinical Medicine Research, Suzhou Research Center of Medical School, Suzhou Hospital, Affiliated Hospital of Medical School, Nanjing University, Suzhou 215000, Jiangsu, China; ²Department of Intensive Care Unit, Suzhou Research Center of Medical School, Suzhou Hospital, Affiliated Hospital of Medical School, Nanjing University, Suzhou 215000, Jiangsu, China. *Equal contributors.

Received March 3, 2024; Accepted August 6, 2024; Epub August 25, 2024; Published August 30, 2024

Abstract: Aberrant RSP01 expression is implicated in tumor progression across various cancers and correlates with anti-cancer immune cell characteristics. However, the specific role of R-spondin 1 (RSP01) in lung adenocarcinoma (LUAD) remains unclear. In this study, we utilized data from The Cancer Genome Atlas (TCGA) to assess RSP01 expression across 33 tumor types. Kaplan-Meier (K-M) analysis revealed the prognostic significance of RSP01 in various cancers. Using statistical software R, we examined RSP01's associations with immune cell infiltration, methylation, mutation, and competing endogenous RNA (ceRNA) networks. Exploration via the Tumor Immune Single Cell Hub (TISCH) database uncovered RSP01's link to the tumor microenvironment (TME) and identified potential small molecule drug targets. We further investigated RSP01's impact on LUAD cell proliferation, metastasis, and the Wnt pathway *in vitro*. Our findings highlight RSP01's role in cancer progression and suggest its potential as both a prognostic marker and therapeutic target in LUAD, implicating the modulation of the Wnt pathway.

Keywords: RSP01, pan-cancer, lung adenocarcinoma, prognostic, immunological

Introduction

The global morbidity and mortality rates of malignant tumors have been staggering in recent years, posing a significant threat to human well-being in this century [1]. Despite recent declines in cancer mortality in developed countries due to advancements in prevention and control technologies, cancer mortality worldwide continues to rise significantly [2]. Many researchers have begun to focus on the common features of various human malignant tumors and delve into the underlying mechanisms of tumor occurrence [3]. Recently, there has been extensive use of pan-cancer investigations to uncover signaling pathways and tumor molecular indicators, aiming to gain a deeper understanding of the molecular mechanisms underlying tumor development [4, 5]. The tumor microenvironment (TME) represented a multifaceted and evolving landscape, consisting of immune cells, vasculature, signaling

entities, and the extracellular matrix surrounding the tumor [6]. Immune checkpoints are intricately connected with various immune cells within the TME, including regulatory T cells (Tregs) and B cells [7]. Therefore, our aim is to identify immunotherapy target that can elucidate the underlying mechanisms of tumors.

RSP01, a member of the R-spondin protein family (RSP01-4), is an agonist of the classic Wnt/ β -catenin pathway and is also considered a regulator of tumor occurrence and progression [8]. Some studies suggest that RSP01 gene expression is upregulated at the beginning of embryonic gonadal sexual differentiation in various species [9]. Hence, RSP01 may accelerate gonadal differentiation, suppress male differentiation processes, and sustain oocyte survival. There is evidence to suggest that RSP01 exhibits abnormal expression trends in various tumor types. For instance, in contrast to normal tissues, LUAD patients have

markedly lower RSP01 expression [10]. Currently, there has been limited systematic research concerning RSP01 in pan-cancer, particularly in LUAD.

In this study, the expression levels of RSP01 and their implications for cancer prognosis were analyzed using R statistical software. This study expanded to include a thorough exploration of the CeRNA networks and pathways linked to RSP01, leveraging resources such as Gene Ontology (GO) and Kyoto Encyclopedia of Genes and Genomes (KEGG) for the analysis. A pronounced connection was observed between the expression of RSP01 and key elements such as immune cell infiltration, the presence of immune checkpoint biomolecules, and responses to immunotherapeutic interventions within the tumor's ecological niche. RSP01 was detected across various immune system components within the TME. Our study further explored the interplay between RSP01 expression and immune-related attributes in LUAD samples, using the TISIDB database for this analysis. This study aims to offer a novel perspective on RSP01 as a prognostic and immunotherapeutic biomarker in pan-cancer, particularly focusing on the biological function of RSP01 within LUAD cells. Furthermore, lab-based studies reveal that heightened RSP01 levels reduce LUAD's growth and metastatic potential by influencing the Wnt signaling cascade.

Material and methods

Data collection

FPKM expression profile and the clinical information of 33 types of tumors as well as LUAD methylation data were extracted from TCGA database. GSE40791 dataset was downloaded from the GEO database.

Differential expression and prognostic value analysis of RSP01

Differential RSP01 protein expressions between tumor tissues and corresponding normal samples were compared using the Wilcoxon rank sum test. We evaluated these differences through immunohistochemical staining, referencing the Human Protein Atlas (HPA) database. To categorize tumors based on RSP01 expression levels, we utilized the

“SurvMiner” and “Survival” software packages. Data were segmented into high and low expression groups based on the median RSP01 expression across various tumors. Survival curves were generated using Kaplan-Meier (K-M) method, and statistical evaluations were performed using the log-rank test.

RSP01 expression and its association with clinical parameters

The diagnostic utility of RSP01 across various tumors was estimated using receiver operating characteristic (ROC) curve analysis.

Protein network establishment and gene enrichment analyses

The STRING database (<https://cn.string-db.org/>) [11] identifies genes with similar functions based on genomic and proteomic data. We utilized the STRING database to identify genes with functions similar to RSP01. Additionally, the WebGestalt Database [12] was employed for KEGG and GO analyses of potential RSP01-related molecules.

Association of RSP01 with immunoregulatory genes in various cancers

The co-expression patterns of RSP01 with a range of genes involved in immune regulation, including immunosuppressors, immunoenhancers, and tumor-infiltrating lymphocytes, across various types of cancers were explored using the data in the TISIDB database [13].

Link between RSP01 and immune cell infiltration in LUAD

The interaction between RSP01 and immune cell infiltration in LUAD tumors was evaluated using the Tumor Immune Estimation Resource (TIMER).

Analysis of RSP01 expression, methylation, and gene mutation

We analyzed differences in RSP01 methylation between LUAD and normal tissue samples using the UALCAN database [14]. Additionally, levels of 12 RSP01 methylation sites were analyzed using R language. We further explored the prognostic value of these RSP01 methylation sites. CBioportal served as a platform for

analyzing the genomic characteristics of RSPO1 in tumors, including mutation frequencies in LUAD [15], encompassing mutations, amplifications, and deep deletions.

The CeRNA network in LUAD

We used the miRanda, miRDB, and TargetScan databases to predict the miRNA targets of RSPO1, while the SpongeScan database was employed to predict its lncRNA targets.

Cell culture

H1299 cells (Fuheng Biology, Shanghai, China) and BEAS-2B cells (BeNa Culture Collection, Suzhou, China) were LUAD cells and normal cells, respectively. Both cell lines were cultured in RPMI 1640 medium (provided by Biosharp, based in Shanghai, China), supplemented with FBS (Hyclone) and streptomycin and penicillin under 5% CO₂ at 37°C.

RNA isolation and qRT-PCR

Total RNA was extracted using Trizol reagent. The purity of RNA samples was assessed, and the reverse transcription was carried out using HiScript II Q RT SuperMix (produced by Vazyme, located in China, catalog number R223-01). qRT-PCR was performed using SYBR qPCR Master Mix (supplied by Vazyme, China, catalog number Q711-02) and a 7500 Fast Real-Time PCR System (manufactured by Applied Biosystems, based in Singapore). The primer sequences used were as follows: RSPO1 Forward: 5'-TGGAGAGGAACGACATCG-3' and Reverse: 5'-CCTTACACTTGGTGCA-GAAGTTA-3'; and β -actin Forward: 5'-GCACCACACCTTCTACAATGAGC-3' and Reverse: 5'-GGATAGCACAGCCTGGATAGCAAC-3'.

Plasmids and shRNA

RSPO1 plasmid was purchased from Public Protein/Plasmid Library Corporation (www.genepl.com). Plasmid transfection was conducted using Lipofectamine 2000 (Invitrogen, USA). To suppress RSPO1 expression, a shRNA sequence specifically targeting RSPO1 was cloned into lentiviral pLKO.1 vector, which was subsequently co-transfected with the psPAX2 packaging plasmid and the pMD2.G envelope plasmid in 293T cells. After a 48-hour incubation, lentivirus expressing RSPO1-targeted shRNA was harvested and used to

infect H1299 cells. The shRNA sequence designed by Public Protein/Plasmid Library was as follows: shRNA sequences: PPL029-54-3a: 5'-TGCTGGCTCTCGAAGACGCAA-3', PPL02954-3b: 5'-CCTGCTGGAGAGGAACGACAT-3', PPL02954-3c: 5'-CAGCCATAACTTCTGCACCAA-3'.

Western blot

RIPA lysis buffer containing 1% PMSF (Biosharp, Shanghai, China) and 1% phosphatase inhibitor (Biosharp, Shanghai, China) was used to extract total protein from H1299 and BEAS-2B cells in following the manufacturer's protocol. Western blotting was performed following the standard protocols to assess protein expression levels in the cells. The antibodies against RSPO1 (Immunoway, USA, YM0566, 1:1000) and α -tubulin (Immunoway, USA, YM3035, 1:1000) were used, and protein signals were detected using an ECL kit (Noblebio, Shanghai, China).

Cell proliferation assay

We used an EdU assay kit to assess the effect of RSPO1 on H1299 cell proliferation following the manufacturer's instructions. Briefly, cells were seeded on coverslips in 24-well plates (2×10^5 cells per well). For EdU incorporation, cells in each well were treated with EdU (Beyotime, Shanghai, China) for 2 hours. Subsequently, cells were fixed with 4% paraformaldehyde for 30 minutes and permeabilized with 0.5% Triton-X-100. The Click-It reaction mixture was applied for 30 minutes in the dark for staining. DAPI was used for nuclear counterstaining. Cell examination was conducted using fluorescence microscopy (Olympus, Suzhou, China), and images were captured with an attached camera.

Wound healing assay

H1299 cells were cultured in 6-well plates until they reached full confluence. After 24 hours of serum deprivation, a sterile 200 μ l pipette tip was used to create a scratch in the cell monolayer. The cell surface was gently washed once with PBS to remove cell debris, followed by addition of serum-free medium to each well. Images of the migrating cells at the same location were captured using an inverted microscope (Olympus, Suzhou, China) equipped with a digital camera at 0, 12, 24 and 48 hours aft-

er scratching, to measure the migrated distance. The mobility of each group was analyzed using Image Analyzer 7.0 software (TechVision Corp., USA).

Transwell migration and invasion assay

The effect of RSP01 on the migratory ability of H1299 cells was assessed using a transwell chamber (Corning Costar, USA) with an 8.0 μm pore polycarbonate membrane. For invasion assay, the chamber was coated with 100 μl of Matrigel (Corning, USA) overnight at 4°C, and then placed in 24-well plates. The bottom chamber was filled with 800 μl of medium containing 10% FBS, while 1×10^5 cells suspended in 200 μl of serum-free RPMI-1640 medium were added to the top chamber for incubation. After 24 hours of incubation, non-migrated cells on the top membrane were removed, and cells that had migrated through the membrane were fixed with 4% paraformaldehyde at room temperature for 20 minutes, followed by staining with 0.5% crystal violet solution for 5 minutes. Cell counts were then recorded.

Statistical analysis

Data are presented as mean \pm SD. Statistical analyses were performed using GraphPad Prism 9 (USA). Comparisons between two groups or more were conducted using Student's t-test or one-way ANOVA, with statistical significance defined as $P < 0.05$.

Results

RSP01 is differentially expressed in pancreatic cancer

RSP01 mRNA levels were assessed across various cancers using RNA sequencing data from 33 different tumor types in TCGA. This analysis revealed a significant decrease in RSP01 mRNA expression in 16 different cancer types, as shown in **Figure 1A**. Furthermore, comparative analysis of paired samples indicated reduced RSP01 expression in tumor tissues, depicted in **Figure 1B**. Data from the HPA database confirmed low RSP01 expression in several cancer types, including LUAD, BLCA, COAD, LIHC, KICH, CESC, PRAD, READ, STAD, and UCEC, illustrated in **Figure 1C**. Overall, RSP01 expression was consistently lower across a majority of cancer types.

Prognostic relevance of RSP01 in various cancer types

Survival correlation analyses focused on overall survival (OS) and disease-specific survival (DSS). The Cox proportional hazards model revealed significant associations between RSP01 expression and OS in MESO ($P < 0.001$), PCPG ($P < 0.001$), HNSC ($P = 0.003$), LUAD ($P = 0.032$), and PRAD ($P = 0.047$), as depicted in **Figure 2A**. RSP01 was identified as a high-risk gene in PCPG but a low-risk gene in HNSC, LUAD, MESO, and PRAD, notably in LUAD (hazard ratio = 0.506). Conversely, higher RSP01 expression correlated with longer survival in HNSC ($P < 0.001$), LGG ($P < 0.001$), MESO ($P < 0.001$), and LUAD ($P = 0.002$) patients. However, in ACC ($P = 0.041$), TGCT ($P = 0.047$), and KIRP ($P = 0.004$) patients, higher RSP01 levels were associated with shorter OS, as shown in **Figure 2B**.

Furthermore, analysis of DSS data (**Figure 2C**) indicated that RSP01 expression correlated with worse prognosis in COAD ($P = 0.035$) and PCPG ($P < 0.001$) patients. Conversely, in HNSC ($P = 0.005$), LUAD ($P = 0.011$), and MESO ($P = 0.003$), higher RSP01 expression was associated with better prognosis. Increased RSP01 expression also correlated with better prognosis in LUAD ($P = 0.017$), LUSC ($P = 0.015$), and LGG ($P < 0.001$) patients, as illustrated in **Figure 2D**.

Clinical relevance analysis of RSP01 in various tumor types

RSP01 expression was associated with pathological in various cancers, including BLCA, BRCA, HNSC, LUAD, LUSC, and STAD (**Figure 3A**). To assess the predictive accuracy of RSP01 across different cancer types, an area analysis under the survival curve analysis was conducted, demonstrating relatively accurate predictive ability for BLCA, BRCA, HNSC, LUAD, LUSC, and STAD (**Figure 3B**). In evaluating RSP01's clinical utility in lung cancer management, a nomogram was developed to predict OS in LUAD patients. This prognostic model integrated RSP01 expression levels with pathological T, N, and M stages as predictive factors (**Figure 3C**). Calibration curves confirmed the nomogram's accuracy in estimating 1-, 3-, and 5-year OS probabilities based on RSP01 expression status (**Figure 3D**). These findings

RSP01 in cancer roles

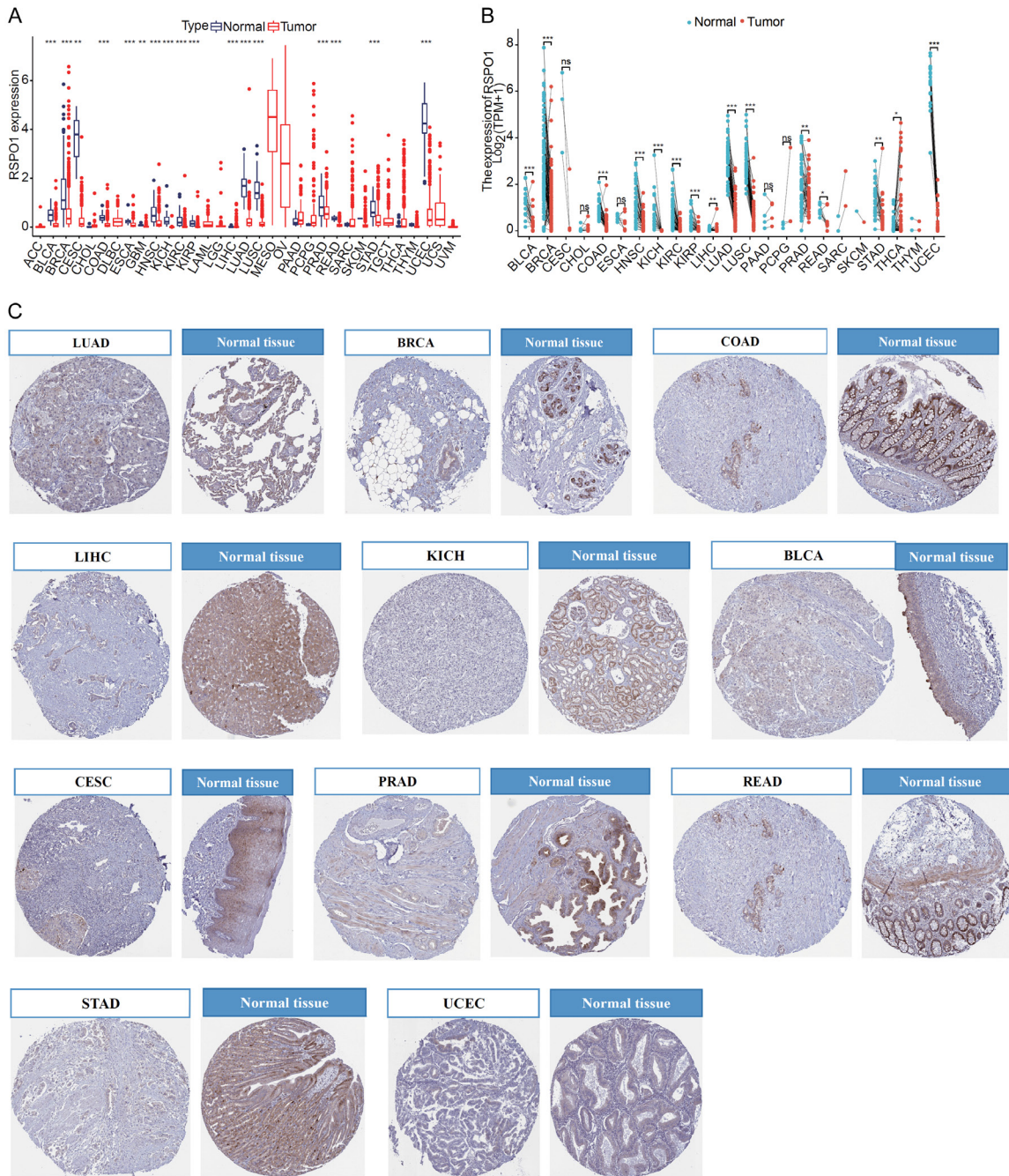


Figure 1. Analysis of differential expression of RSP01. A. The expression of RSP01 mRNA in pan-cancer. B. Paired analysis compared the expression differences of RSP01 in tumors and corresponding adjacent tissues. Analysis using Mann Whitney U test, ns, $P \geq 0.05$; * $P < 0.05$; ** $P < 0.01$; *** $P < 0.001$. C. RSP01 expression in pan-cancer from the HPA database.

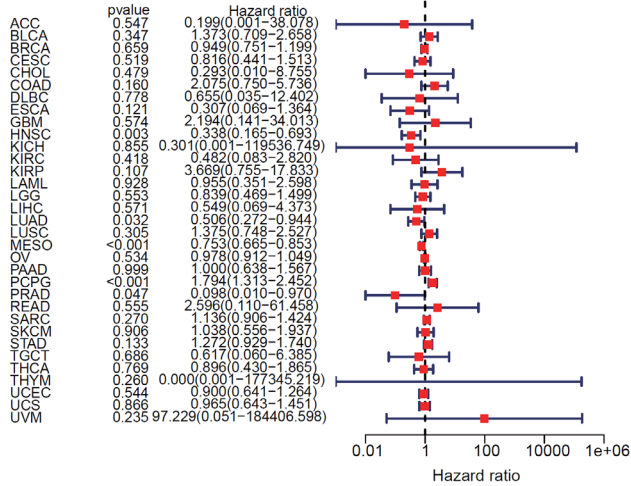
indicated that the RSP01-integrated nomogram, combining molecular and traditional pathological staging factors, offers reliable prognostic evaluation in LUAD patients. Considering prognosis, clinical staging, ROC analysis, and OS results, RSP01 showed promising predictive performance in LUAD.

RSP01 co-expression molecular network and enrichment analyses

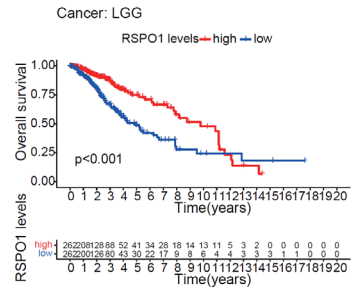
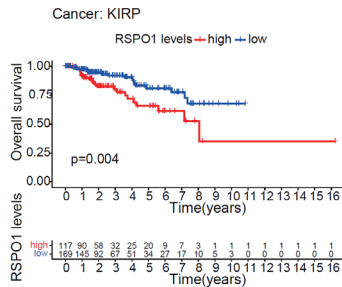
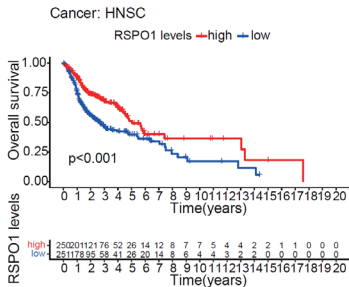
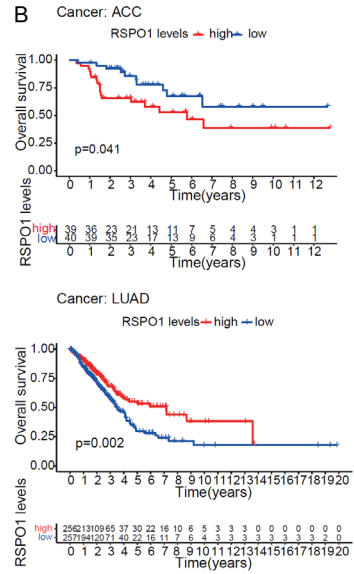
To gain insights into the potential functions of RSP01, we conducted an analysis of RSP01 interacting molecules using STRING ([Figure S1A](#)). To explore the involvement of RSP01 and

RSPO1 in cancer roles

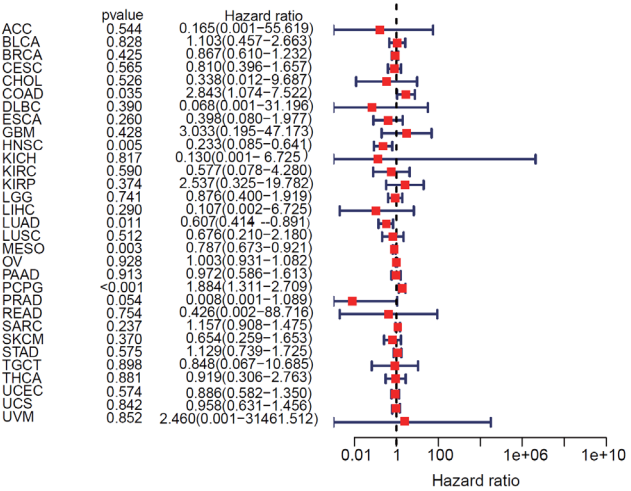
A



B



C



D

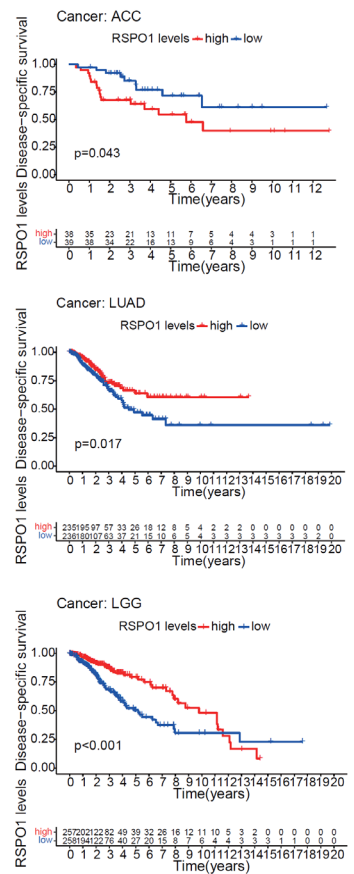


Figure 2. Correlation between RSPO1 expression and survival time. A. Forest map of OS correlation among 33 types of tumors. B. Kaplan-Meier analyzed the relationship between RSPO1 expression and OS. C. Forest map of DSS correlation among 33 forms of tumors. D. Kaplan-Meier analyzed the relationship of RSPO1 expression with DSS.

its co-expressed molecules, we performed KEGG and GO analyses. The GO analysis revealed significant enrichment in three primary domains: biological process (BP) such as cell communication, response to stimuli, and biological regulation; molecular function (MF) including protein binding and molecular transducer activity; and cellular component (CC) mainly involving membrane and endomembrane systems (Figure S1B). KEGG pathway analysis identified associations with pathways such as basal cell carcinoma, the Wnt signaling, breast cancer, gastric cancer, and the mTOR signaling pathway (Figure S1C). GSEA indicated functional enrichment in processes like alditol NADP+ oxidoreductase activity, aminoglycoside antibiotic metabolic process, and miRNA catabolic process. Additionally, KEGG pathway analysis highlighted connections to arrhythmogenic right ventricular cardiomyopathy and cell adhesion molecules (CAMs) (Figure S2). These findings underscore the significant involvement of RSPO1 in key pathways such as Wnt and mTOR signaling, emphasizing its relevance in tumorigenesis.

Correlation of RSPO1 with immunomodulatory-related genes in pan-cancer

Elevated RSPO1 levels are positively correlate with increased tumor-infiltrating immune cells, as depicted in Figure S3A. Specifically in LUAD, eosinophils ($R = 0.567$, $P = 2.2e-16$) and mast cells ($R = 0.577$, $P = 2.2e-16$) were identified as the predominant types of tumor-infiltrating lymphocytes (TILs) (Figure S3B). Additionally, RSPO1 expression showed a positive correlation with the presence of immunoinhibitory factors, as illustrated in Figure S3C. In LUAD, prominent immunoinhibitors correlating with RSPO1 included ADORA2A ($R = 0.356$, $P = 5.52e-17$) and BTLA ($R = 0.375$, $P = 2.2e-16$) (Figure S3D).

Furthermore, RSPO1 expression was positively associated with immunomodulatory elements (Figure S3E). In LUAD, prominent immunomodulators included CXCL12 ($R = 0.559$, $P < 2.2e-16$) and CD40LG ($R = 0.484$, $P < 2.2e-16$) (Figure S3F). In the final phase of our research,

we investigated the relationship between RSPO1 expression and both tumor mutational burden (TMB) and microsatellite instability (MSI), which are indicative of immune checkpoint inhibitor (ICI) efficacy. Across various cancers, RSPO1 levels showed a notable inverse relationship with TMB (Figure S3G). Additionally, RSPO1 exhibited a negative correlation with MSI in LUSC, MESO, STAD, UCEC, CHOL, ESCA, NHSC, and LIHC (Figure S3H).

Link between RSPO1 and immune cell infiltration in LUAD

The expression of RSPO1 showed positive correlation with the presence of resting mast cells, resting memory CD4+ T cells, memory B cells, resting dendritic cells, and monocytes. Conversely, RSPO1 expression inversely correlated with the presence of activated memory CD4+ T cells, activated mast cells, resting natural killer cells, and follicular helper T cells (Figure 4A, 4B). These variations in immune cell infiltration levels appeared to correspond with alterations in the copy number variation of RSPO1. Specifically, in LUAD, the infiltration levels of CD4+ T cells, CD8+ T cells, macrophages, and neutrophils were associated with RSPO1 copy number variations. These findings underscore a strong relationship between RSPO1 copy number alterations and variations in immune cell infiltration (Figure 4C). To deepen our understanding of the interplay between RSPO1 expression and the TME in LUAD, we utilized the CIBERSORT algorithm to analyze TICs within LUAD samples. Initially, we compared the composition of twenty-two immune cell types between samples with high and low RSPO1 expression, revealing significant differences in seven types of TICs (Figure 4D). Given that the TME comprises tumor cells, immune cells, and stromal cells, our subsequent analysis focused on the relationship between RSPO1 expression and various TME scores. We found a positive correlation between RSPO1 expression and ESTIMATE score, immune score, and stromal score in LUAD (as shown in Figure 4E). Because of the crucial role of immune checkpoint (ICP) proteins in cancer immunotherapy, particularly in regulat-

RSP01 in cancer roles

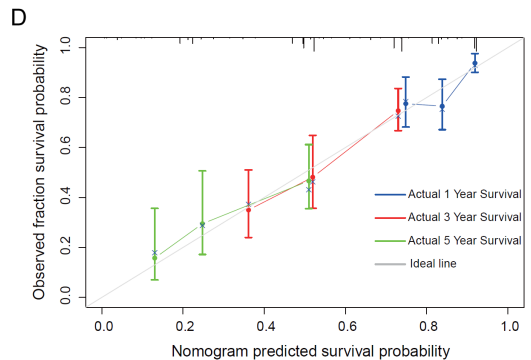
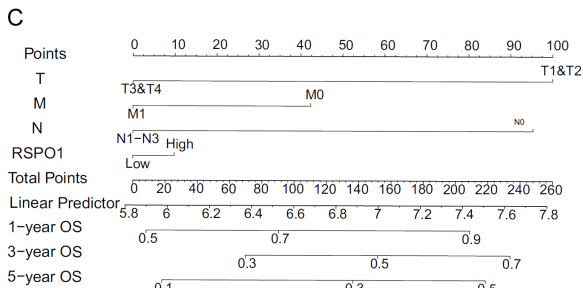
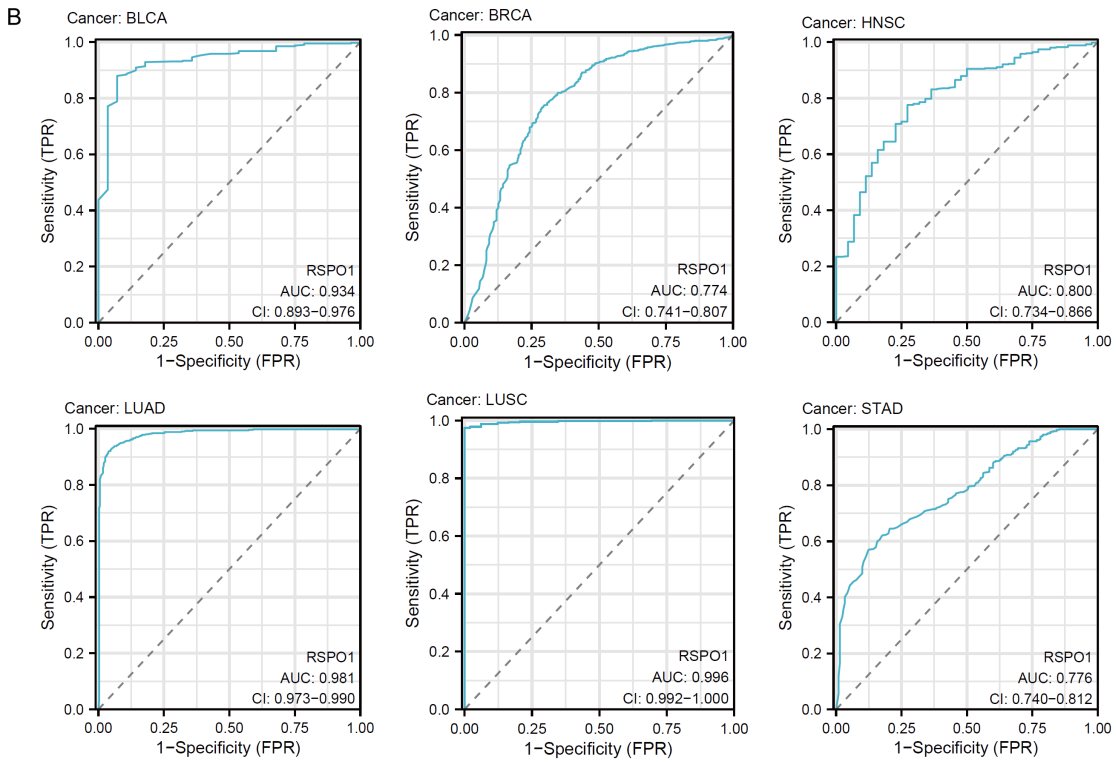
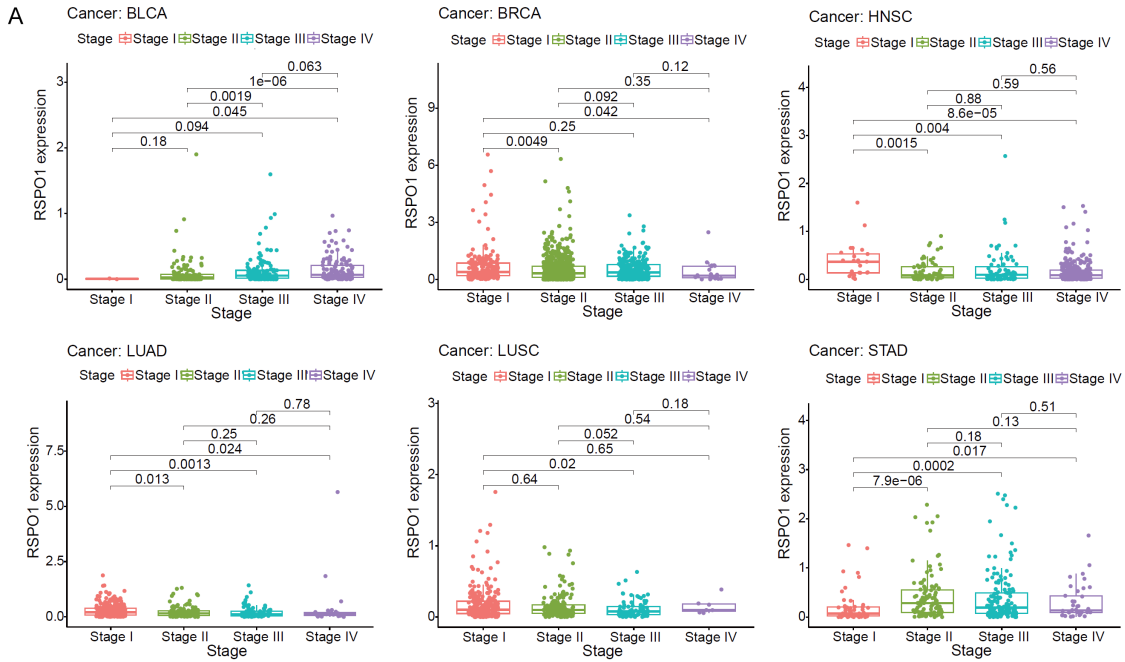


Figure 3. Clinical relevance analysis of RSP01 of different tumors. A. Correlation of RSP01 expression with tumor stage in different tumors. B. Area analysis under the survival curve of RSP01 in various tumors. C. Construction of a nomogram model for RSP01 utilizing TCGA datasets. D. Calibration curves for the nomogram model at 1, 3, and 5 years.

ing immune cell infiltration within the TME, we investigated the association between ICP gene expression levels and RSP01 expression in LUAD. Our study revealed a positive correlation between RSP01 expression and immune checkpoint genes in LUAD (**Figure 4F**), suggesting RSP01 may influence the efficacy of immunotherapeutic strategies targeting these checkpoints. We employed the Tumor Immune Dysfunction and Exclusion (TIDE) metric to evaluate tumor immune dysfunction and potential immune evasion based on tumor sample expression profiles. Our findings indicated that tumors with higher RSP01 expression levels exhibited increased potential for immune escape, potentially reducing the effectiveness of immune checkpoint inhibitor (ICI) therapy (**Figure 4G**). Additionally, we assessed the efficacy of ICIs using the Immunophenotype Score (IPS). Our results showed that patients in the high-risk group, based on RSP01 expression, tended to have a slightly higher IPS compared to those in the low-risk group when treated with CTLA4 and PD1 blockers (**Figure 4H-K**). This suggests nuanced differences in therapeutic response to these therapies based on risk stratification.

Prognostic value of RSP01 methylation

To evaluate the prognostic value of RSP01 methylation, we first determined the methylation levels of RSP01 in LUAD and normal tissue samples (**Figure S4A**). Our analysis identified 12 CpG sites with RSP01 methylation (**Figure S4B**), and a significantly negative correlation was observed between RSP01 mRNA expression and the methylation level of the CpG site cg22063989 (**Figure S4C**). Furthermore, we found that the expression of the cg22063989 CpG in LUAD was associated with a better prognosis (**Figure S4D**).

Genomic aberrations such as mutations, deletions, and amplifications in oncogenes or tumor suppressor genes significantly contribute to the development and progression of various cancers. To gain a comprehensive understanding of these genomic alterations, we conducted an extensive examination of genetic alterations in the RSP01 gene. Utilizing data from TCGA

and the resources available on the cBioPortal platform, our investigation encompassed a range of genetic disruptions in RSP01, including mutations, structural variations, gene amplifications, and significant deletions. This information elucidates the impact and implications of RSP01 alterations in cancer initiation and progression. The most prevalent genetic alteration observed in the RSP01 gene was amplification in OV. Additionally, mutations were detected in LUAD, UCEC, and SKCM. A significant proportion of PCPG samples exhibited missing data for the RSP01 gene (**Figure S4E**). An examination of data from the cBioPortal database identified missense mutations as the predominant form of RSP01 gene mutation in cancerous tumors (**Figure S4F**). We then further investigated the association between RSP01 expression and specific genomic characteristics, focusing on somatic mutations and copy number variations (CNVs) within the TCGA-LUAD dataset. In this analysis, the group with high RSP01 expression (n = 248) displayed a more frequent occurrence of somatic mutations in genes such as TP53 (42%), TTN (42%), MUC16 (38%), and CSMD3 (33%). In contrast, the group with low RSP01 expression (n = 254) showed a higher incidence of somatic mutations in TP53 (49%), TTN (35%), MUC16 (41%), and CSMD3 (42%) (**Figure S4G** and **S4H**). These findings demonstrate a substantial association between RSP01 expression levels and the occurrence of specific somatic mutations and copy number variations in tumors.

The CeRNA network in LUAD

We downloaded the miRNAs predicted for RSP01 from miRanda, miRDB, and TargetScan, and identified 5 miRNA-mRNA pairs from their intersection (**Figure S5A**). We then conducted survival analysis on these 5 miRNAs and found that only hsa-miR-432-3p and hsa-miR-592 had prognostic value (**Figure S5B**). Additionally, 4 lncRNAs were identified as miRNA targets using the SpongeScan database. We visualized the CeRNA network for mRNA, miRNA, and lncRNA by using Cytoscape (**Figure S5C**). The results indicated that the upstream regulatory

RSP01 in cancer roles

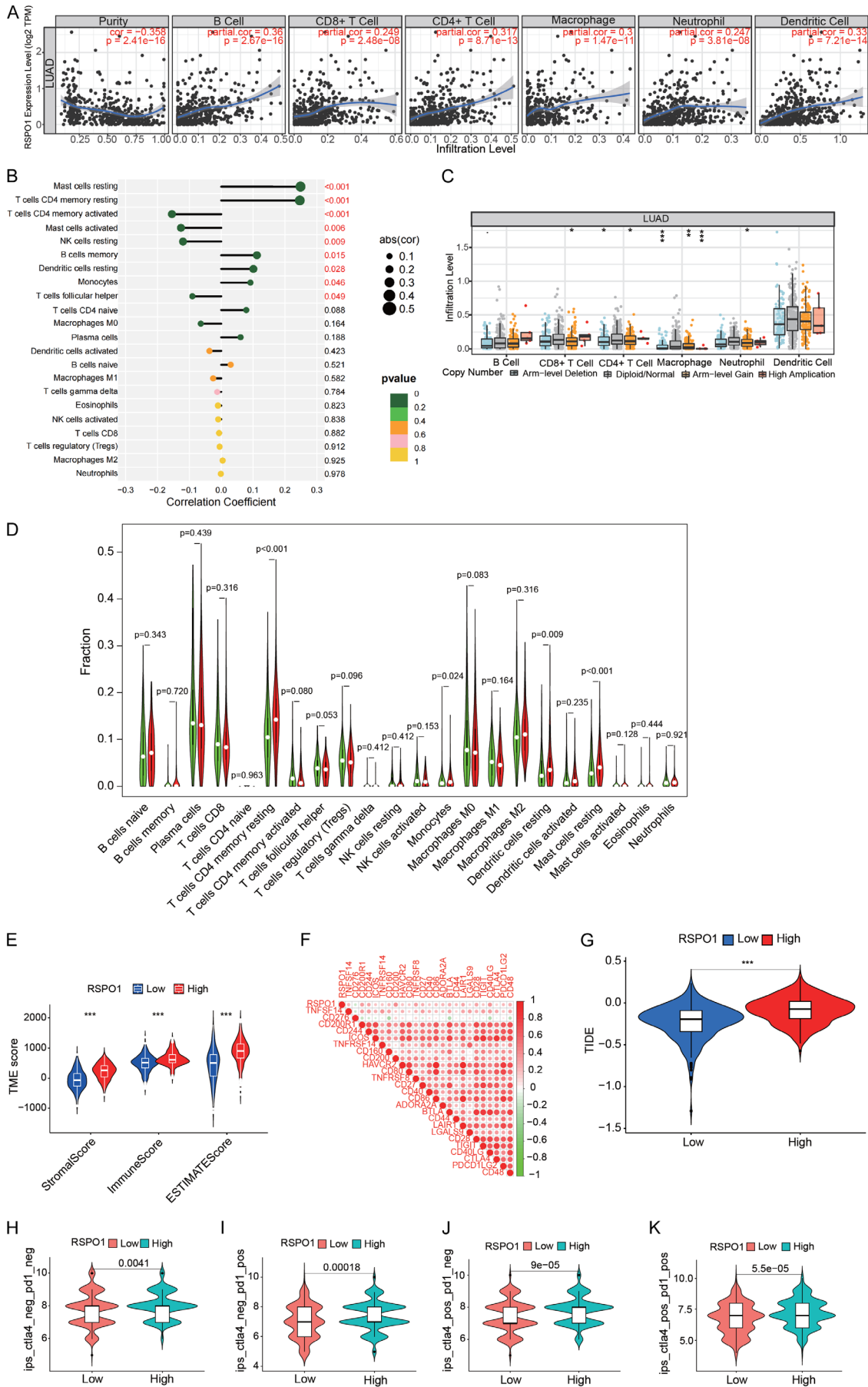


Figure 4. Correlation between RSP01 and immune cell infiltration. A. The expression of RSP01 in LUAD tissues is related to immune cell infiltration. B. The relationship between RSP01 expression and 22 types of tumor infiltrating lymphocytes. C. RSP01 copy number variation affects the infiltration level of immune cells in LUAD. D. Compare the proportion of RSP01 high expression group and low expression group in 22 immune cell types. E. The immune infiltration level of RSP01 expression group in StromalScore, ImmuneScore and ESTIMATEScore. F. RSP01 was associated with tumor immune checkpoint molecules. G. Compare the TIDE levels between the RSP01 high expression group and the low expression group. H-K. The relationship between IPS and RSP01 high-low expression groups in LUAD patients.

network of lncRNA-miRNA might regulate the abnormal expression of RSP01 in LUAD.

Correlation between RSP01 and TME heterogeneity

We used two datasets from the TISCH database (GSE131907 and GSE149655) to evaluate the expression of RSP01 in TME-related immune cells. In the GSE131907, we identified 12 cell types, with CD4+ T cells having the highest cell count ($n = 42763$) (Figure S6A, S6B). RSP01 expression was found only in fibroblasts and was low (Figure S6C). We verified this expression in fibroblasts using an external dataset, yielding consistent results (Figure S7). In the GSE149655 dataset, we identified 9 cell types, with alveolar cells being the most numerous ($n = 3,578$) (Figure S6D, S6E). RSP01 was again only expressed in fibroblasts and at low level (Figure S6F). These findings suggested significant variations in RSP01 expression across different cell types, with fibroblasts in LUAD displaying the highest expression level. This observation may contribute to the heterogeneity observed in the LUAD microenvironment, highlighting the importance of cell-type-specific expression patterns in tumor biology.

Drug sensitive prediction based on RSP01 expression

The correlation between RSP01 levels and drug sensitivity based on CTRP data indicated that WZ4002 (an EGFR inhibitor) and dexamethasone (a glucocorticoid receptor agonist) were the top two drugs positively correlated with RSP01 expression (Figure S8A). Conversely, GANT-61 (a GLI antagonist) and UNC-0638 (a histone lysine methyltransferase inhibitor) were the top two drugs negatively correlated with RSP01 expression (Figure S8A). Additionally, the correlation analysis using the GDSC dataset showed that BMS-754807 (an IGF-1R inhibitor), SB216763 (a GSK-3 inhibi-

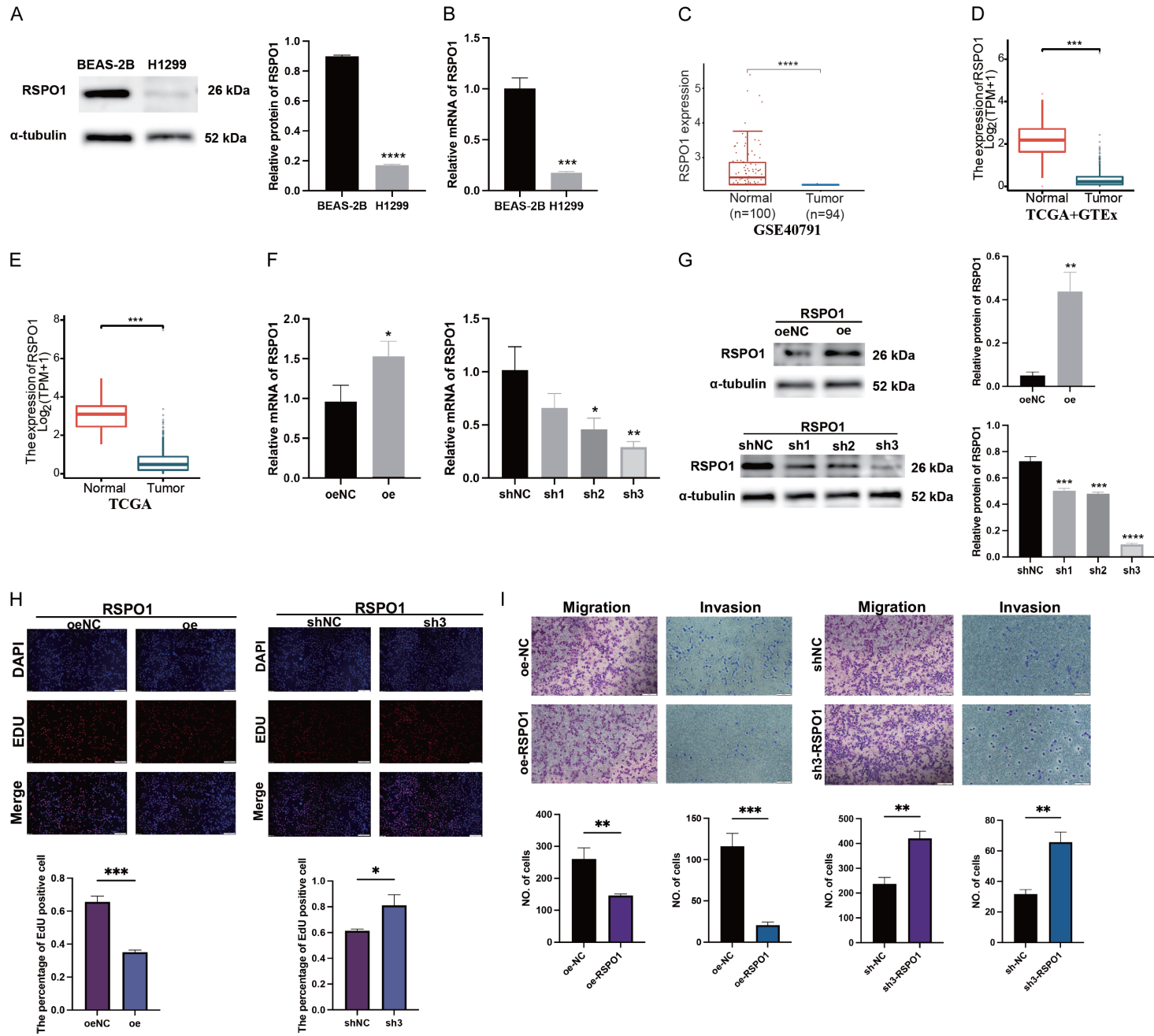
tor), and doramapimod were the top three drugs correlated with RSP01 expression (Figure S8B). These results suggest potential targeted small molecule drugs with therapeutic effects, providing a theoretical basis for clinical treatment targeting RSP01.

Effect of RSP01 downregulation on LUAD cell growth

To explore whether RSP01 was dysregulated in LUAD, we assess mRNA and protein expression of RSP01 in H1299 and BEAS-2B cells. Western blot results indicated that RSP01 was downregulated in H1299 cells compared to BEAS-2B cells (Figure 5A). Additionally, qRT-PCR results were consistent with protein expression levels (Figure 5B). We further confirmed the consistent expression levels using data from three databases (Figure 5C-E). Verification of mRNA expression in the GSE116959, GSE115002 and GSE134381 datasets also aligned with the protein expression results (Figure S9).

To experimentally demonstrate the effects of RSP01 dysregulation in cell behavior, we overexpressed or knocked down RSP01 by shRNA in H1299 cells. RT-PCR and Western blot analysis confirmed the successful overexpression or knockdown at mRNA and protein levels, respectively (Figure 5F, 5G). The results indicated that the knockout efficiency was highest with the sh1-RSP01, hence the carrier was named as shRSP01. The EdU incorporation assay showed that inhibiting RSP01 expression in H1299 cells promoted cell proliferation, while upregulating RSP01 expression inhibited cell proliferation (Figure 5H). Furthermore, transwell assays revealed that upregulation of RSP01 expression decreased the migratory and invasive abilities of H1299 cells, whereas silencing RSP01 expression facilitated these abilities (Figure 5I). Additionally, cell scratch experiments demonstrated that RSP01 knockdown H1299 cells exhibited markedly enhanced

RSP01 in cancer roles



RSPO1 in cancer roles

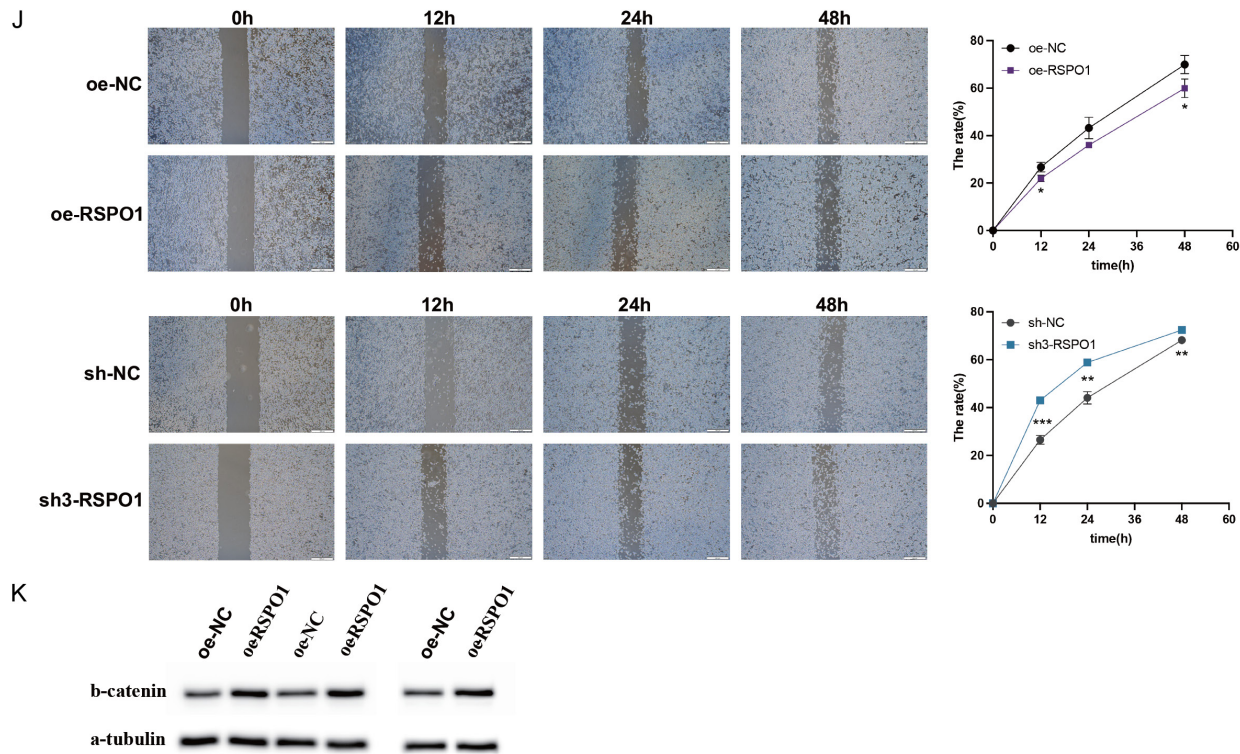


Figure 5. RSPO1 was downregulated in LUAD cell. Weston blot (A) and qRT-PCR (B) determine RSPO1 expression between H1299 cells and BEAS-2B cells. (C-E) Represents the expression of RSPO1 in the TCGA and GSE40791 datasets. Detection of overexpression and knockdown efficiency of RSPO1 in H1299 cells using qRT-PCR (F) and Weston blot (G), respectively. (H) EDU proliferation assay. (I) Effect of RSPO1 upregulation and downregulation on the invasive and migratory capacities of H1299 cells utilizing transwell assay. (J) Detection of Cell migration by cell scratch assay. (K) The effect of RSPO1 overexpression on WNT signaling marker expression was assessed by western blot.

healing ability, while RSPO1-overexpressing H1299 cells showed clearly weakened healing ability (**Figure 5J**). The expression of β -catenin, a key protein of Wnt pathway, was higher in RSPO1 group than in the control group (**Figure 5K**). These findings demonstrated that RSPO1 overexpression inhibits invasion and migration of LUAD, whereas its downregulation facilitated invasion and migration of LUAD.

Discussion

Pan-cancer analysis helps identify similarities and differences among various tumors, facilitate the discovery of new treatment and prognostic markers, and provides novel insights into cancer prevention and treatment [16]. Despite progress in LUAD treatment, it remains one of the most malignant cancers with a poor 5-year survival rate [17]. Thus, discovering novel biomarkers and exploring their mechanisms is crucial. Our study investigated the role of RSPO1 in various tumors, with a focus on LUAD, analyzing its prognostic value, tumor immunity, and methylation. We also explored the upstream lncRNA-miRNA network regulating RSPO1 expression in LUAD and its effects on tumor progression. In vitro experiments showed that RSPO1 overexpression suppresses the proliferation and migratory capabilities of LUAD cells and modulates the Wnt signaling pathway. These findings offer valuable insights into RSPO1's potential role in regulating tumor growth and metastasis.

RSPO1 overexpression through the Wnt/ β -catenin signaling pathway significantly suppresses mitochondrial respiration and heat production in adipocytes, contributing to human obesity [18]. SiRNA RSPO1 has been shown to reduce cellular proliferative and migratory in ovarian cancer and to induce apoptosis [19]. The GO results revealed that the pathways associated with RSPO1 are primarily enriched in cell communication, response to stimuli, biological regulation, membrane and endomembrane systems, and protein binding. KEGG analysis identified significant enrichment in pathways related to the Wnt and mTOR signaling pathways. Our research demonstrated that RSPO1 overexpression leads to increased expression of β -catenin compared to the control group, which aligns with our analysis results. This suggests that RSPO1 may influ-

ence the biological behavior of LUAD primarily through its interaction with the Wnt signaling pathway, highlighting a potential mechanism by which RSPO1 modulates cancer progression, particularly in LUAD.

The composition and interplay of immune cells, cytokines, and chemokines within the tumor immune microenvironment play a crucial role in orchestrating tumorigenesis as well as the processes of cancer metastasis (20, 21). This underscores the importance of further exploring the relationship between RSPO1 and the infiltration of immune cells associated with tumors. Tumor neoantigens have been shown to regulate the function of tumor-specific CD4+ T cells by facilitating their interaction with tumor-specific B cells, which ultimately enhances the functionality of CD8+ T cells and promotes anti-tumor immunity (22).

TAGAP's role in modulating the differentiation and function of CD4+ T cells in LUAD through the STAT pathway is significant, as it contributes to increased immune infiltration and cytotoxicity (23). In vitro studies have shown that THBS2 recombinant protein can inhibit T cell proliferation, while in vivo studies have demonstrated its support for LUAD growth and distant micrometastasis (24). Furthermore, research has indicated that immune scores are reliable predictors of survival, likelihood of metastasis, and resistance to therapy in cancer patients (25).

Our study demonstrated that RSPO1 expression positively correlates with both matrix and immune scores in LUAD, highlighting its interactions with tumor and immune cells in this cancer type (26). Additionally, genes related to immune checkpoints are crucial targets for ICIs, which are recognized as effective strategies in cancer immunotherapy (26). We analyzed RSPO1 and immune-associated genes (immunoinhibitors, immunostimulators, TILs) across various cancers. In BLCA, CHOL, HNSC, LUAD, LUSC, PAAD, and PRAD, most immune-related genes and immune cells showed a positively correlation with RSPO1. Conversely, in SARC and TGCT, most immune-related genes were negatively correlated with RSPO1. Notably, RSPO1 expression was positively related to several key immune checkpoints, including CD200R1, CD200, TNFRSF8, and CD40LG. This suggests that RSPO1 could

be a novel target for cancer immunotherapy. Furthermore, our research revealed a significant association between RSPO1 and immune regulatory genes, indicating RSPO1's substantial role in immune infiltration of tumor cells and positioning it as a promising candidate for developing new immunosuppressive treatments.

RNA methylation, a key epigenetic process, plays a crucial role in determining patient outcomes. This process encompasses various types of modifications, including m5C, m6A, and Nm. In the context of LUAD, hypermethylation of RSPO1 has been positively correlated with improved progression-free survival, consistent with the more favorable outcomes observed in patients with lower RSPO1 mRNA levels.

The interaction between protein-encoded mRNA and non-coding RNA functions is established through CeRNA network, which is significant in the pathogenesis of diseases [20, 21]. We identified miRNAs and lncRNAs targeting RSPO1 using platforms such as Targetscan, miWalk, and miRDB, and established lncRNA-miRNA-RSPO1 regulatory networks to regulate aberrant RSPO1 expression in various cancers. Research suggests that hsa-miR-592 has an anti-tumor effect in NSCLC by inhibiting the activity of SOX9 [22]. Additionally, hsa-miR-592 inhibits ovarian cancer cell growth by targeting ERBB3 [23]. Both studies suggest that Hsa-miR-592 may inhibit the growth of lung and ovarian cancer tumors. Conversely, CircASCC3-mediated miR-432 increases complement C5a levels, promoting NSCLC progression and dysfunctional immune status [24]. This suggests that hsa-miR-432-3p/hsa-miR-592 axis might inhibit the proliferation, migration, and metastasis of LUAD through RSPO1 overexpression. Our findings suggest that hsa-miR-432-3p/hsa-miR-592-RSPO1 network could be a potential mechanism in LUAD. Moreover, in vitro experiments demonstrated that RSPO1, as a tumor suppressor gene, suppresses cellular growth, invasion, and migration in LUAD.

Our research has some limitations. Firstly, while RSPO1 expression was associated with tumor immunity and methylation based on public database, additional experimental validation is needed. Furthermore, conducting further functional assays using multiple shRNAs is cru-

cial to fully exclude off-target effects and enhance the robustness of our conclusions. These assays would provide deeper insights into the specific mechanisms by which RSPO1 influences the proliferative, migratory, and invasive behaviors of LUAD cells. Moreover, the specific mechanisms by which RSPO1 modulates the proliferative, migratory, and invasive abilities of LUAD cells remain uncertain. Future studies will focus on exploring the essential signaling pathways and targets of RSPO1 in regulating these cellular behaviors, which will provide a theoretical foundation for understanding RSPO1's role in LUAD progression and its potential as an effective treatment target.

In summary, our findings indicate that RSPO1 exhibits abnormal expression across various cancer types and is significantly correlated with patient prognosis. RSPO1 expression also shows a notable association with tumor immunity in multiple tumors. Therefore, RSPO1 emerges as a promising therapeutic and prognostic biomarker. In vitro experiments confirmed RSPO1's role as a tumor suppressor gene in LUAD. The research suggests that RSPO1 could serve as an underlying prognostic indicator for tumors and play a critical role in the proliferation and metastasis of LUAD.

Acknowledgements

This study was supported by Suzhou Science and Technology Association Youth Science and Technology Talent Support Project (12).

Disclosure of conflict of interest

None.

Address correspondence to: Drs. Mingdeng Wang and Yuansheng Lin, Department of Intensive Care Unit, Suzhou Research Center of Medical School, Suzhou Hospital, Affiliated Hospital of Medical School, Nanjing University, No. 1 Lijiang Road, Suzhou 215000, Jiangsu, China. E-mail: 1376590818@qq.com (MDW); linys202012@163.com (YSL)

References

- [1] Sung H, Ferlay J, Siegel RL, Laversanne M, Soerjomataram I, Jemal A and Bray F. Global cancer statistics 2020: GLOBOCAN estimates of incidence and mortality worldwide for 36 cancers in 185 countries. *CA Cancer J Clin* 2021; 71: 209-249.

- [2] Santucci C, Carioli G, Bertuccio P, Malvezzi M, Pastorino U, Boffetta P, Negri E, Bosetti C and La Vecchia C. Progress in cancer mortality, incidence, and survival: a global overview. *Eur J Cancer Prev* 2020; 29: 367-381.
- [3] Jin X, Cai Y, Xue G, Que J, Cheng R, Yang Y, Xiao L, Lin X, Xu C, Wang P, Xu Z, Nie H and Jiang Q. Identification of shared characteristics in tumor-infiltrating T cells across 15 cancers. *Mol Ther Nucleic Acids* 2023; 32: 189-202.
- [4] Saidak Z, Soudet S, Lottin M, Salle V, Sevestre MA, Clatot F and Galmiche A. A pan-cancer analysis of the human tumor coagulome and its link to the tumor immune microenvironment. *Cancer Immunol Immunother* 2021; 70: 923-933.
- [5] Wei C, Wang B, Peng D, Zhang X, Li Z, Luo L, He Y, Liang H, Du X, Li S, Zhang S, Zhang Z, Han L and Zhang J. Pan-cancer analysis shows that ALKBH5 is a potential prognostic and immunotherapeutic biomarker for multiple cancer types including gliomas. *Front Immunol* 2022; 13: 849592.
- [6] Taki M, Abiko K, Ukita M, Murakami R, Yamanoi K, Yamaguchi K, Hamanishi J, Baba T, Matsumura N and Mandai M. Tumor immune microenvironment during epithelial-mesenchymal transition. *Clin Cancer Res* 2021; 27: 4669-4679.
- [7] Zhang H, Dai Z, Wu W, Wang Z, Zhang N, Zhang L, Zeng WJ, Liu Z and Cheng Q. Regulatory mechanisms of immune checkpoints PD-L1 and CTLA-4 in cancer. *J Exp Clin Cancer Res* 2021; 40: 184.
- [8] He Z, Zhang J, Ma J, Zhao L, Jin X and Li H. R-spondin family biology and emerging linkages to cancer. *Ann Med* 2023; 55: 428-446.
- [9] Smith CA, Shoemaker CM, Roeszler KN, Queen J, Crews D and Sinclair AH. Cloning and expression of R-Spondin1 in different vertebrates suggests a conserved role in ovarian development. *BMC Dev Biol* 2008; 8: 72.
- [10] Wu L, Zhang W, Qian J, Wu J, Jiang L and Ling C. R-spondin family members as novel biomarkers and prognostic factors in lung cancer. *Oncol Lett* 2019; 18: 4008-4015.
- [11] Zhuang Z, Lin T, Luo L, Zhou W, Wen J, Huang H, Liu Z and Lin L. Exploring the mechanism of aidi injection for lung cancer by network pharmacology approach and molecular docking validation. *Biosci Rep* 2021; 41: BSR20204062.
- [12] Wang J, Vasaikar S, Shi Z, Greer M and Zhang B. WebGestalt 2017: a more comprehensive, powerful, flexible and interactive gene set enrichment analysis toolkit. *Nucleic Acids Res* 2017; 45: W130-W137.
- [13] Huang XY, Liu JJ, Liu X, Wang YH and Xiang W. Bioinformatics analysis of the prognosis and biological significance of VCAN in gastric cancer. *Immun Inflamm Dis* 2021; 9: 547-559.
- [14] Chandrashekar DS, Karthikeyan SK, Korla PK, Patel H, Shovon AR, Athar M, Netto GJ, Qin ZS, Kumar S, Manne U, Creighton CJ and Varambally S. UALCAN: an update to the integrated cancer data analysis platform. *Neoplasia* 2022; 25: 18-27.
- [15] Cerami E, Gao J, Dogrusoz U, Gross BE, Sumer SO, Aksoy BA, Jacobsen A, Byrne CJ, Heuer ML, Larsson E, Antipin Y, Reva B, Goldberg AP, Sander C and Schultz N. The cBio cancer genomics portal: an open platform for exploring multidimensional cancer genomics data. *Cancer Discov* 2012; 2: 401-404.
- [16] Ter Steege EJ and Bakker ERM. The role of R-spondin proteins in cancer biology. *Oncogene* 2021; 40: 6469-6478.
- [17] Shi Y, Xu Y, Xu Z, Wang H, Zhang J, Wu Y, Tang B, Zheng S and Wang K. TKI resistant-based prognostic immune related gene signature in LUAD, in which FSCN1 contributes to tumor progression. *Cancer Lett* 2022; 532: 215583.
- [18] Sun Y, Zhang J, Hong J, Zhang Z, Lu P, Gao A, Ni M, Zhang Z, Yang H, Shen J, Lu J, Xue W, Lv Q, Bi Y, Zeng YA, Gu W, Ning G, Wang W, Liu R and Wang J. Human RSPO1 mutation represses beige adipocyte thermogenesis and contributes to diet-induced adiposity. *Adv Sci (Weinh)* 2023; 10: e2207152.
- [19] Liu Q, Zhao Y, Xing H, Li L, Li R, Dai J, Li Q and Fang S. The role of R-spondin 1 through activating Wnt/ β -catenin in the growth, survival and migration of ovarian cancer cells. *Gene* 2019; 689: 124-130.
- [20] Qi X, Zhang DH, Wu N, Xiao JH, Wang X and Ma W. CeRNA in cancer: possible functions and clinical implications. *J Med Genet* 2015; 52: 710-718.
- [21] Zhang K, Zhang L, Mi Y, Tang Y, Ren F, Liu B, Zhang Y and Zheng P. A ceRNA network and a potential regulatory axis in gastric cancer with different degrees of immune cell infiltration. *Cancer Sci* 2020; 111: 4041-4050.
- [22] Li Z, Li B, Niu L and Ge L. miR-592 functions as a tumor suppressor in human non-small cell lung cancer by targeting SOX9. *Oncol Rep* 2017; 37: 297-304.
- [23] Jin Q, Zhang N, Zhan Y, Xu X, Han C, Zhao H, Hu X, Tang H and Wu Y. MicroRNA-592 inhibits the growth of ovarian cancer cells by targeting ERBB3. *Technol Cancer Res Treat* 2023; 22: 15330338231157156.
- [24] Gao J, Zhang LX, Ao YQ, Jin C, Zhang PF, Wang HK, Wang S, Lin M, Jiang JH and Ding JY. Elevated circASCC3 limits antitumor immunity by sponging miR-432-5p to upregulate C5a in non-small cell lung cancer. *Cancer Lett* 2022; 543: 215774.

RSP01 in cancer roles

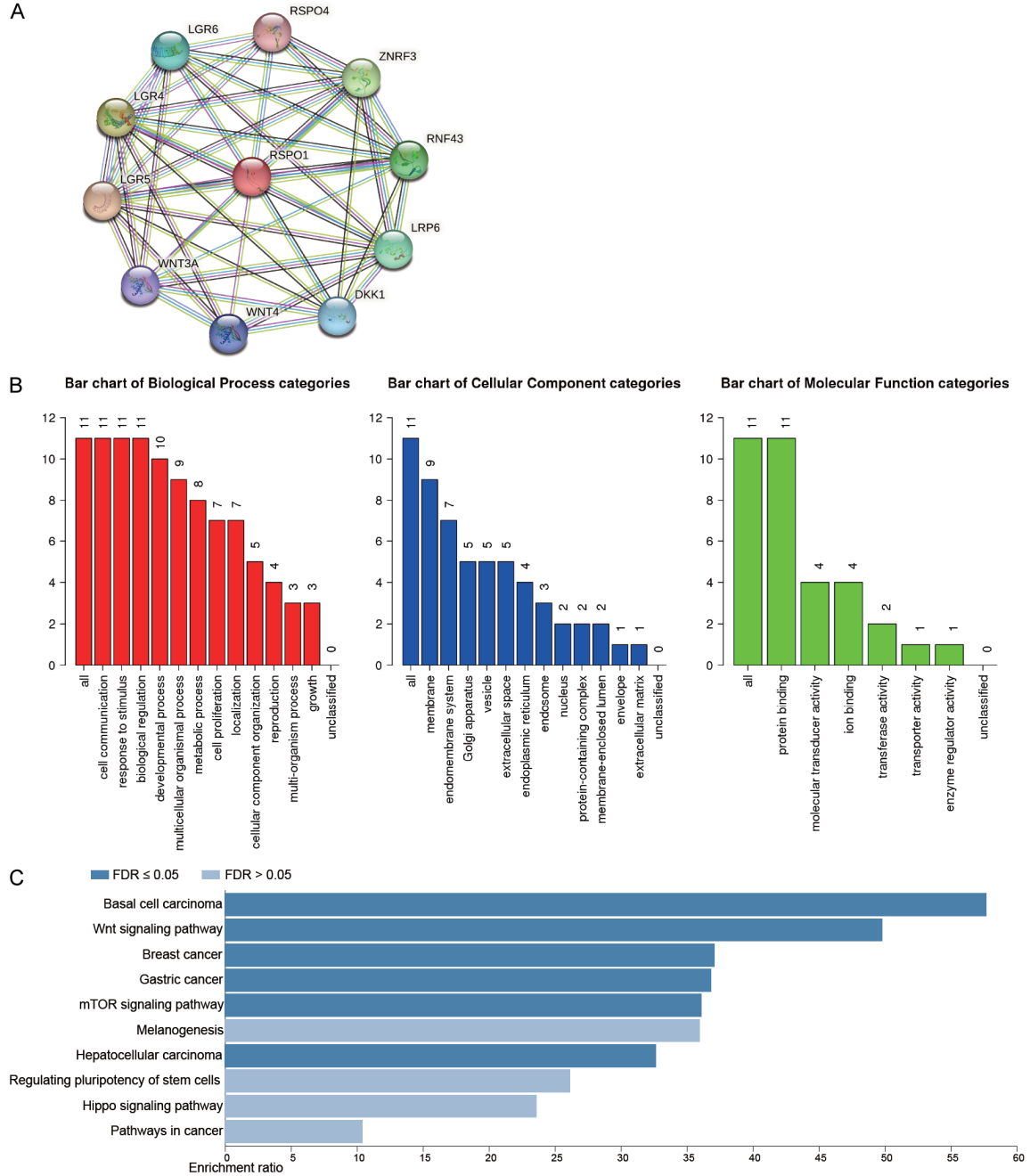


Figure S1. Underlying functions of RSP01. A. Creation of a possible interacting molecular network of RSP01 utilizing STRING. B, C. Enrichment analysis of molecules interacting with RSP01 (GO and KEGG).

RSP01 in cancer roles

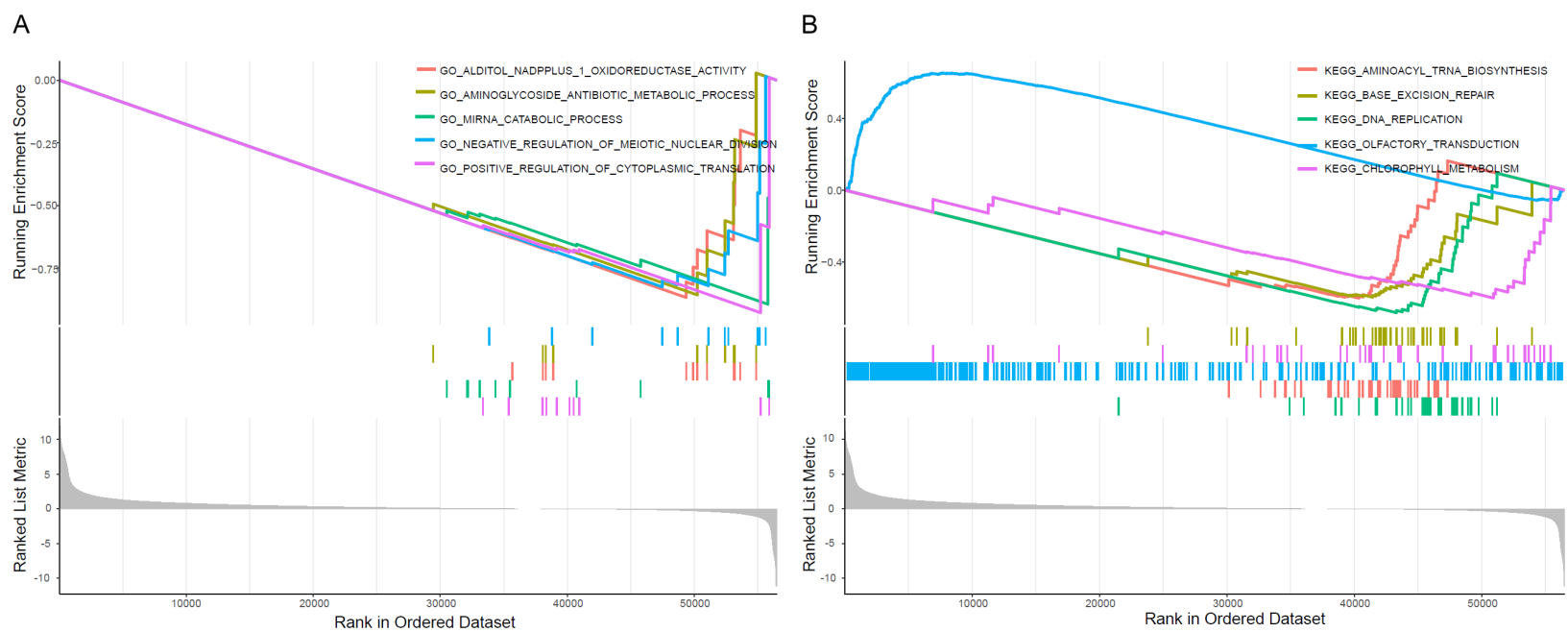
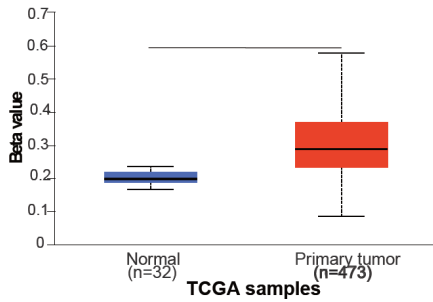


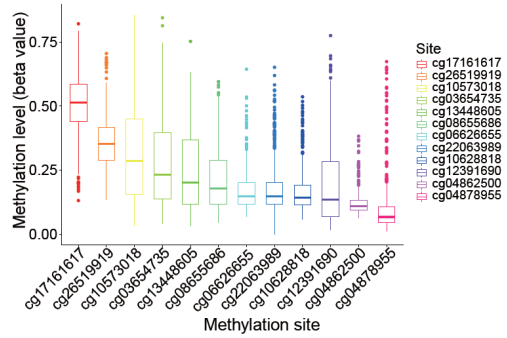
Figure S2. GSEA analysis uncovered the involvement of RSP01 expression in a range of Gene Ontology (GO) terms and Kyoto Encyclopedia of Genes and Genomes (KEGG) pathways.

RSP01 in cancer roles

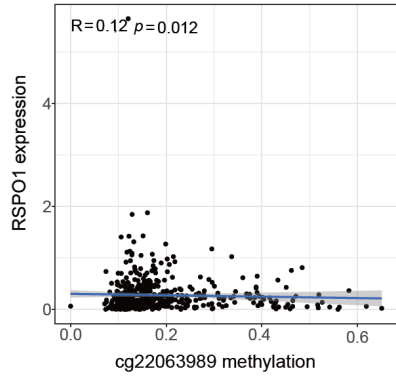
A Promoter methylation level of RSP01 in LUAD



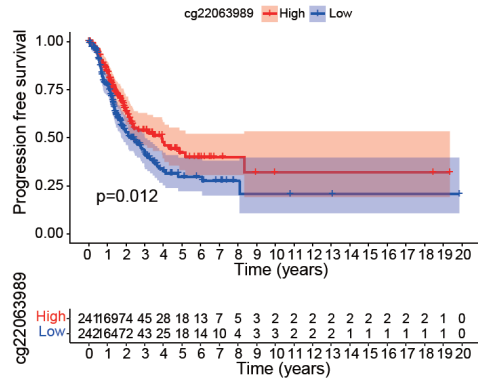
B



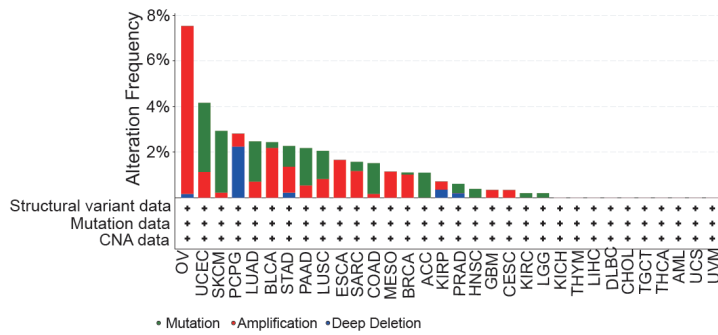
C



D

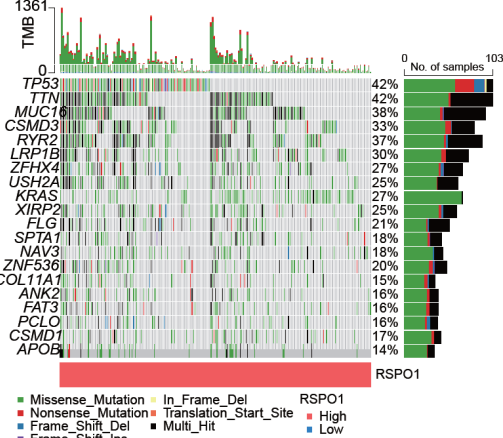


E



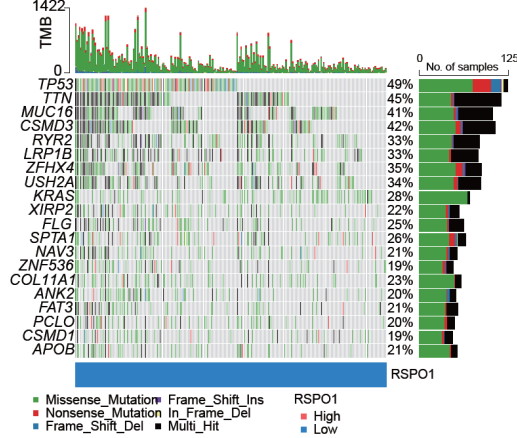
F

Altered in 213 (85.89%) of 248 samples.

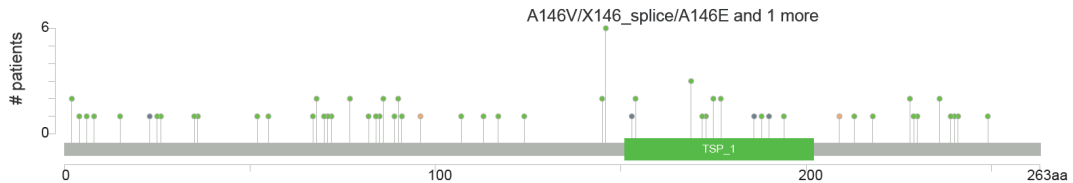


G

Altered in 241 (94.88%) of 254 samples.



H



RSP01 in cancer roles

Figure S4. Bioinformatics analysis of the association of RSP01 expression with methylation in LUAD tissue. (A) Methylation level of RSP01 in healthy and LUAD tissue samples. (B) The distribution of 12 RSP01 methylated CpG sites. (C) cg22063989 methylation negatively regulates the expression of RSP01. (D) Survival analysis of LUAD patients with high and low cg22063989 in TCGA-LUAD dataset. (E) Genetic alterations of RSP01 in pan-cancer through the cBioPortal. (F) The mutation sites of RSP01 in multiple tumors by the cBioPortal tool. (H) Detection of differential somatic mutations in LUAD, including 25% RSP01high group (G) and RSP01low group.

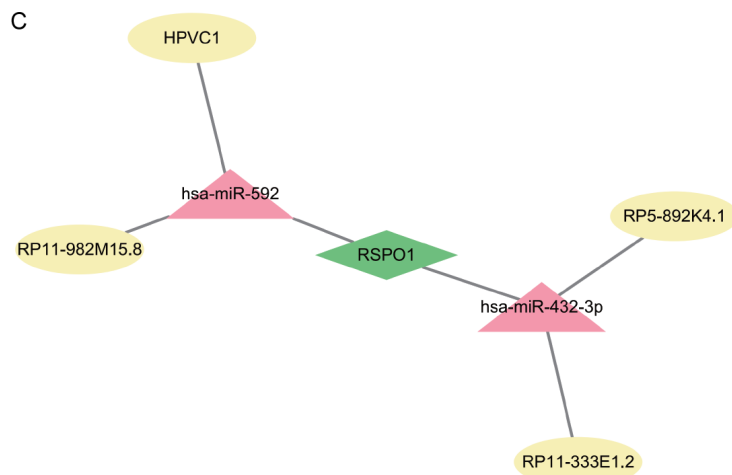
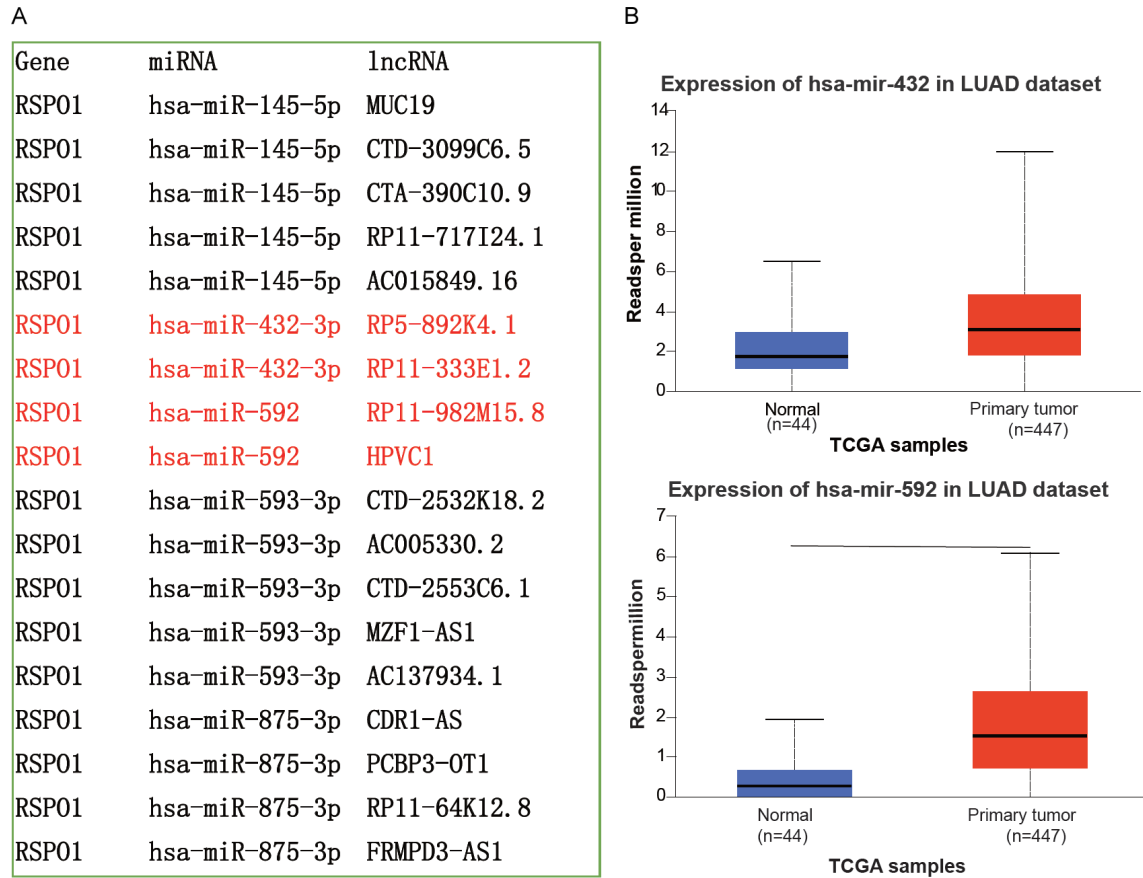


Figure S5. The regulatory network constructed in LUAD. A. Using miRanda, miRDB, and TargetScan databases to predict upstream miRNAs of RSP01, and using SpongeScan database to predict upstream lncRNAs of miRNAs. B. Screening out differentially expressed genes for miRNA. C. The regulatory network constructed through Cytoscape includes RSP01, 2 miRNAs, and 4 lncRNAs.

RSP01 in cancer roles

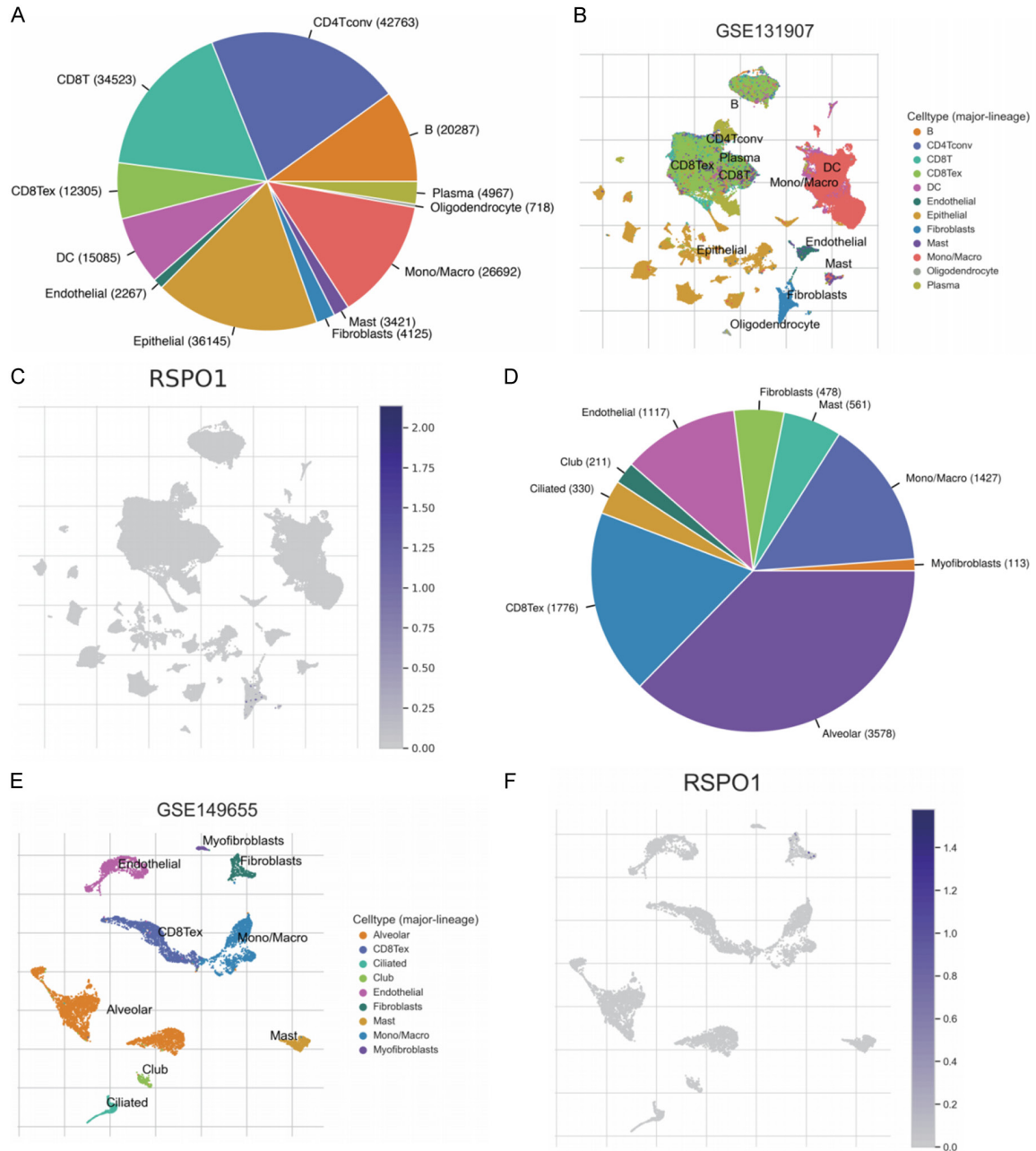


Figure S6. RSP01-related cell type distribution through scRNA-seq database. A, B, D, E. The cell types and their distribution in GSE131907 and GSE149655 datasets. C, F. Distribution of CD47 in different cells in GSE131907 and GSE149655 datasets.

RSP01 in cancer roles

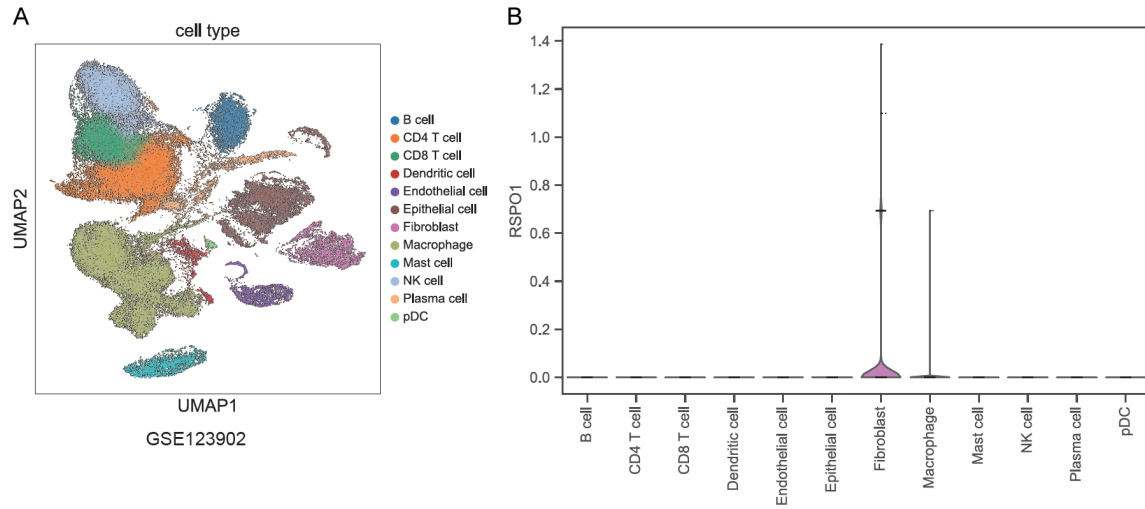


Figure S7. Clustering of LUAD in the GSE123902 dataset and the expression levels of RSP01 across various cell types. A. The visualization of LUAD clustering within the single-cell cohort of the GSE123902 dataset. B. This depiction highlights the expression levels of RSP01 in each cell type.

RSP01 in cancer roles

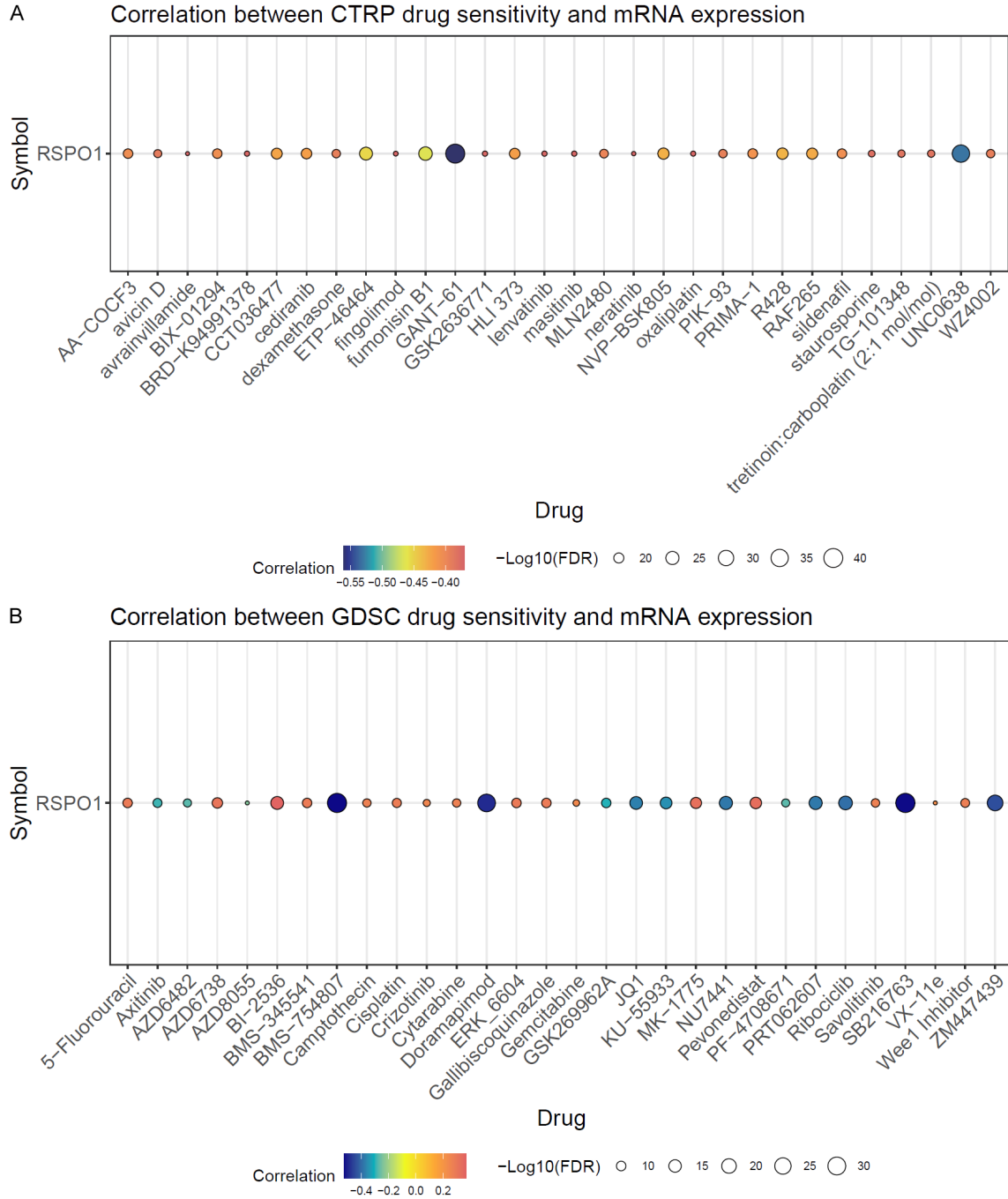


Figure S8. Sensitive drug prediction of RSP01 in LUAD. Predictive drugs based on the RSP01 expression in LUAD from the CTRP (A) and GDSC (B) datasets.

RSP01 in cancer roles

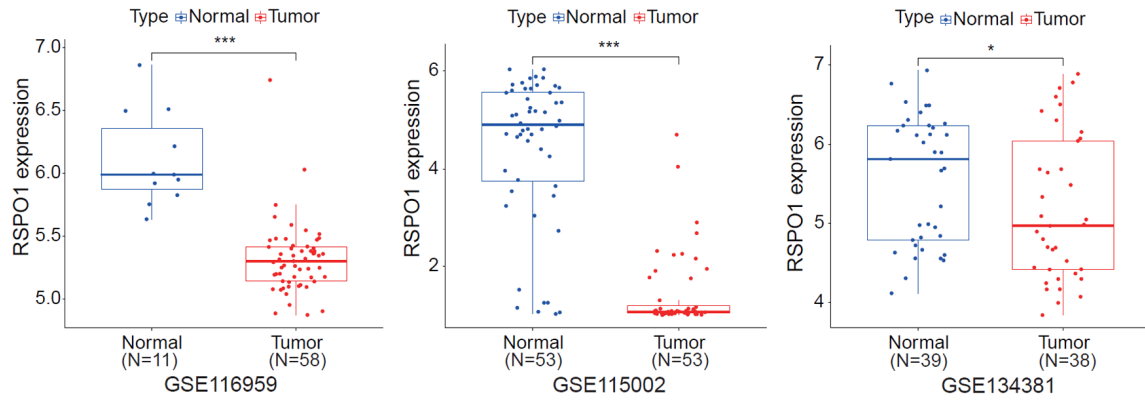


Figure S9. Compare the expression levels of RSP01 between the normal and LUAD groups across the datasets GSE116959, GSE115002, and GSE134381.